Energetic Contributions and Topographical Organization of Ligand Binding Residues of Tissue Factor†

Wolfram Ruf,‡ Curtis R. Kelly,‡ John R. Schullek,‡ David M. A. Martin,§ Igor Polikarpov,|| C. William G. Boys,|| Edward G. D. Tuddenham,§ and Thomas S. Edgington*,‡

Departments of Immunology and Vascular Biology, The Scripps Research Institute, IMM-17, 10666 North Torrey Pines Road, La Jolla, California 92037, Haemostasis Research Group, MRC Clinical Sciences Centre, Royal Postgraduate Medical School, Du Cane Road, London W12 0NN, U.K., and Department of Biochemistry, The Medical School, Hugh Robson Building, George Square, Edinburgh EH8 9XD, U.K.

Received November 10, 1994; Revised Manuscript Received March 7, 1995⊗

ABSTRACT: Tissue factor is the cellular receptor and macromolecular enzymatic cofactor for the serine protease coagulation factor VIIa. The ligand binding extracellular domain of tissue factor consists of two structural modules which fold similar to fibronectin type III modules, consistent with the classification of tissue factor as a member of the class 2 cytokine receptor family. On the basis of the three-dimensional structure, we here analyze the importance of tissue factor residues for binding of ligand by scanning alanine mutagenesis. The identified significant binding contacts account for as much as 80% of the calculated total free energy of ligand binding. Most residues with energetic contributions to ligand binding are well exposed to solvent, and the area for ligand interaction extends from the cleft formed by the two structural modules (residues Lys^{20}, Ile^{22}, Lys^{48}, Asp^{58}, Arg^{135}, Phe^{140}) to the convex-shaped edge of the three- and four-stranded sheets characterized by a patch of surface-exposed hydrophobic side chains in the amino-terminal module (residues Gln^{37}, Asp^{44}, Trp^{45}, Phe^{76}, Tyr^{78}). The binding residues are dispersed over an extended surface area, indicating adaptation to the recognition of specific structural modules of the macromolecular ligand factor VIIa. This analysis provides detailed insight into the three-dimensional organization of the ligand docking structure of the initiating cofactor for the coagulation pathways.

The coagulation pathways *in vivo* are initiated by the cell surface receptor tissue factor (TF)[1] (Davie et al., 1991). TF is thought to play a significant pathogenetic role in vascular and thromboembolic diseases [for review see Ruf and Edgington (1994)]. TF forms a catalytic enzyme−cofactor complex with the serine protease coagulation factor VIIa (VIIa) resulting in significantly enhanced proteolytic activation of the macromolecular substrates factors X and IX. Recently, the three-dimensional structure of the extracellular domain of TF has been solved (Harlos et al., 1994; Muller et al., 1994), demonstrating folding into two fibronectin type III like modules as found in other members of the cytokine receptor family. Binding of VIIa to the extracellular domain modules of TF occurs with high affinity (Waxman et al., 1992) and involves predominantly protein−protein interactions (Schullek et al., 1994). The VIIa light chain modules (Higashi et al., 1994; Toomey et al., 1991; Clarke et al., 1992; Kazama et al., 1993; O'Brien et al., 1994; Ruf et al., 1991a) as well as the serine protease domain (O'Brien et al., 1991; Higashi et al., 1994; Matsushita et al., 1994) are involved in the interaction with TF. Specific amino acid side chains of TF, notably Lys^{20}, Ile^{22}, Asp^{58}, Arg^{135}, and Phe^{140}, have been identified as important for binding of ligand (Ruf et al., 1994), and these five residues account for approximately one-third of the calculated free energy of binding of VIIa by TF (Schullek et al., 1994), indicating that additional structure is involved in ligand docking. We here identify novel TF residues which contribute to binding of ligand. These residues not only interact with ligand independently from the previously characterized contact sites but also mark a spatial extension of the known ligand binding site in TF. The presented integration of the functional analysis with structural data provides novel insight into the organization of the docking structure for the ligand VIIa.

EXPERIMENTAL PROCEDURES

Mutagenesis and Expression of Human, Full-Length TF (TF_{1-263}). Mutants of TF were generated using oligonucleotide-directed mutagenesis, as described in detail (Ruf et al., 1993). Multiple mutations were introduced by annealing two or three nonoverlapping oligonucleotides to the template DNA. Mutated DNA sequences were identified by newly introduced restriction endonuclease cleavage sites, and mutations were confirmed by DNA sequencing. Wild-type and mutant TF were expressed in mammalian Chinese hamster ovary cells (CHO-K1) in transient transfection experiments. Cells were harvested after 48 h, TF concentration was determined by immunoassay (Ruf et al., 1993), and cell pellets were stored at −70 °C in aliquots until functional analysis. The expression of monoclonal antibody epitopes was analyzed by inhibition assay (Ruf et al., 1994) and by

† This work was supported by National Institutes of Health Grant P01 HL 16411. Computer services were provided by the GCRC facilities and supported by NIH Grant M01 RR 00833. E.G.D.T. is supported by the Medical Research Council and C.W.G.B. by the Wellcome Trust. D.M.A.M. is the recipient of a Medical Research Council studentship.

‡ The Scripps Research Institute.
§ Royal Postgraduate Medical School.
|| The Medical School.

⊗ Abstract published in *Advance ACS Abstracts,* May 1, 1995.

[1] Abbreviations: TF, tissue factor; VIIa, factor VIIa; CHO cell, Chinese hamster ovary cell.

0006-2960/95/0434-6310$09.00/0

flow cytometry (Ruf et al., 1993), when stably transfected cell lines were available.

K_{Dapp} Determination by Enzyme-Linked Functional Assay. The apparent dissociation constant (K_{Dapp}) for binding of VIIa by TF was determined in a functional assay reporting proteolytic activation of the substrate factor X to quantify the formation of TF·VIIa complexes, as described in detail previously (Ruf et al., 1994; Schullek et al., 1994). Briefly, cells were lysed by vortexing in the presence of 15 mM octyl β-D-glucopyranoside (Calbiochem, San Diego, CA) in HBS (20 mM HEPES, 130 mM NaCl, pH 7.4), followed by incubation at 37 °C for 15 min and a final dilution of 1:3 with HBS (Ruf et al., 1993). For determination of the K_{Dapp}, TF·VIIa complexes were allowed to form at 37 °C for 10 min in HBS, 5 mM $CaCl_2$, and 0.5% bovine serum albumin, followed by the addition of factor X (100 nM) to quantify TF·VIIa complex formation. Factor Xa generation was determined with chromogenic substrate. The maximum catalytic rate was calculated from linear double-reciprocal plots of rate versus concentration of VIIa including only concentrations of VIIa which are in excess of the fixed concentration of TF. The rates observed were converted to concentrations of TF·VIIa complexes based on the maximum catalytic rate at the fixed TF concentration in the assay. Free ligand was calculated by subtracting the bound VIIa from the initial VIIa concentration in the assay. Binding parameters K_{Dapp} and B_{max} were obtained by fitting the data to the single-site binding equation using the program Enzfitter (Elsevier Biosoft). Scatchard plots demonstrated a linear fit of the data for the mutants characterized in this study. The free energy of binding was calculated from the K_{Dapp} according to the formula $\Delta G = -RT \ln(1/K_{Dapp})$ with a temperature of 37 °C.

Localization of Residues in the Structure of TF. The three-dimensional structure of the TF extracellular domain has recently been solved by crystallography (Harlos et al., 1994). The spatial organization of the residue side chains in the three-dimensional structure was analyzed on a Silicon Graphics Personal Iris using Insight II (Biosym, San Diego, CA). Accessible surface area was calculated using the program DSSP (Kabsch & Sander, 1983). The calculations used the van der Waals radii for all atoms with a probe radius of 1.4 Å.

RESULTS

Spatial Alignment of Ligand Binding Residues at the Module Boundary. The recently solved crystal structure of the TF extracellular domain (Harlos et al., 1994) provided an opportunity to evaluate the spatial organization of the binding site for the macromolecular ligand VIIa. Previous analysis from our laboratory has defined three major independent contacts which are provided by residues Ile^{22}, Lys^{20}/Asp^{58}, and Arg^{135}/Phe^{140} (Schullek et al., 1994). These five residues are exposed to solvent (Table 1) and located at the module boundary with Lys^{20}, Ile^{22}, and Asp^{58} forming a continuous cluster on the surface of the amino-terminal module (Figure 1). Leu^{133} is filling space between this cluster and the carboxy-terminal residue Phe^{140}. The Ala double exchange mutant at the Leu^{133}/Val^{134} position had slightly reduced affinity for VIIa [$\Delta\Delta G$ < 0.5 kcal/mol (Ruf et al., 1994)], suggesting that the exposed Leu^{133} side chain makes subtle contributions to a continuous area for ligand binding at the module boundary.

Table 1: Accessible Surface Area for Residues Discussed in This Study

residue	accessible surface area (Å²)	residue	accessible surface area (Å²)
Lys^{20}	125	Asp^{54}	94
Ile^{22}	31	Glu^{56}	94
Glu^{24}	64	Asp^{58}	60
Val^{33}	22	Thr^{60}	3
Val^{36}	0	Asp^{61}	102
Gln^{37}	34	Glu^{62}	28
Ile^{38}	5	Lys^{65}	139
Thr^{40}	41	Lys^{68}	121
Gly^{43}	29	Phe^{76}	23
Asp^{44}	146	Tyr^{78}	54
Trp^{45}	69	Pro^{92}	57
Lys^{46}	101	Tyr^{94}	109
Ser^{47}	33	Arg^{131}	179
Lys^{48}	61	Leu^{133}	70
Cys^{49}	31	Arg^{135}	144
Phe^{50}	112	Arg^{136}	126
Tyr^{51}	129	Asn^{138}	160
Thr^{53}	90	Phe^{140}	102

We had previously characterized a TF mutant (Trp^{45}/Ser^{47}→Arg/Gly) which had no apparent structural alterations and normal function by coagulation assay (Rehemtulla et al., 1992). Determination of the K_{Dapp} by functional titration assay demonstrated a 10-fold decreased affinity for binding of VIIa (Table 2), consistent with the previous observation that the relatively high concentration of VII in plasma can mask reduction in TF binding function (Ruf et al., 1994). The loss of binding function is attributable to the Trp^{45} exchange, based on individual Ala replacement mutants (Table 2). These data provided evidence that the ligand binding region extends to a fairly remote contact point on the surface of the amino-terminal module of the TF extracellular domain (Figure 1).

Contributions of the Hydrophobic Cluster Residues to VIIa Binding. Trp^{45} is part of a hydrophobic surface cluster which also includes the aromatic side chains of Phe^{50}, Tyr^{51}, Phe^{76}, and Tyr^{94}, as well as the aliphatic side chains of Val^{33} and Pro^{92} (Figure 2). Previous analysis excluded Phe^{50} as a contact residue for VIIa binding (Ruf et al., 1994). We analyzed whether additional residues in this region are involved in interaction with VIIa by generating individual Ala replacements at the respective positions. Tyr^{51}, Tyr^{94}, Val^{33}, and Pro^{92} exhibited normal binding of VIIa, but the K_{Dapp} of VIIa binding for Phe^{76} and Tyr^{78} was increased 6- and 3-fold, respectively (Table 2). There was no evidence for a reduction in binding of conformation-dependent monoclonal antibodies to the mutants, consistent with the concept that Ala replacements for surface-exposed residues (Table 1) are without effect on global folding of proteins. The decreased binding of VIIa by the Trp^{45}, Phe^{76}, and Tyr^{78} exchange mutants thus likely reflects loss of ligand contact, suggesting extension of the ligand interface to the convex-shaped surface area at the edge of the three- and four-stranded sheets (Figure 2).

Identification of Novel Binding Residues in the Amino-Terminal Module of TF. The surface between the hydrophobic residues and the major docking site at the module boundary is predominantly shaped by the side chains of residues Asp^{44}, Gln^{37}, Ser^{47}, Lys^{46}, Lys^{48}, Cys^{49}, Asp^{61}, and Lys^{65} (Figure 3). The Asp^{44}→Ala exchange resulted in a similar loss of binding as the Trp^{45} replacement, whereas the Gly^{43}→Ala substitution was compatible with normal

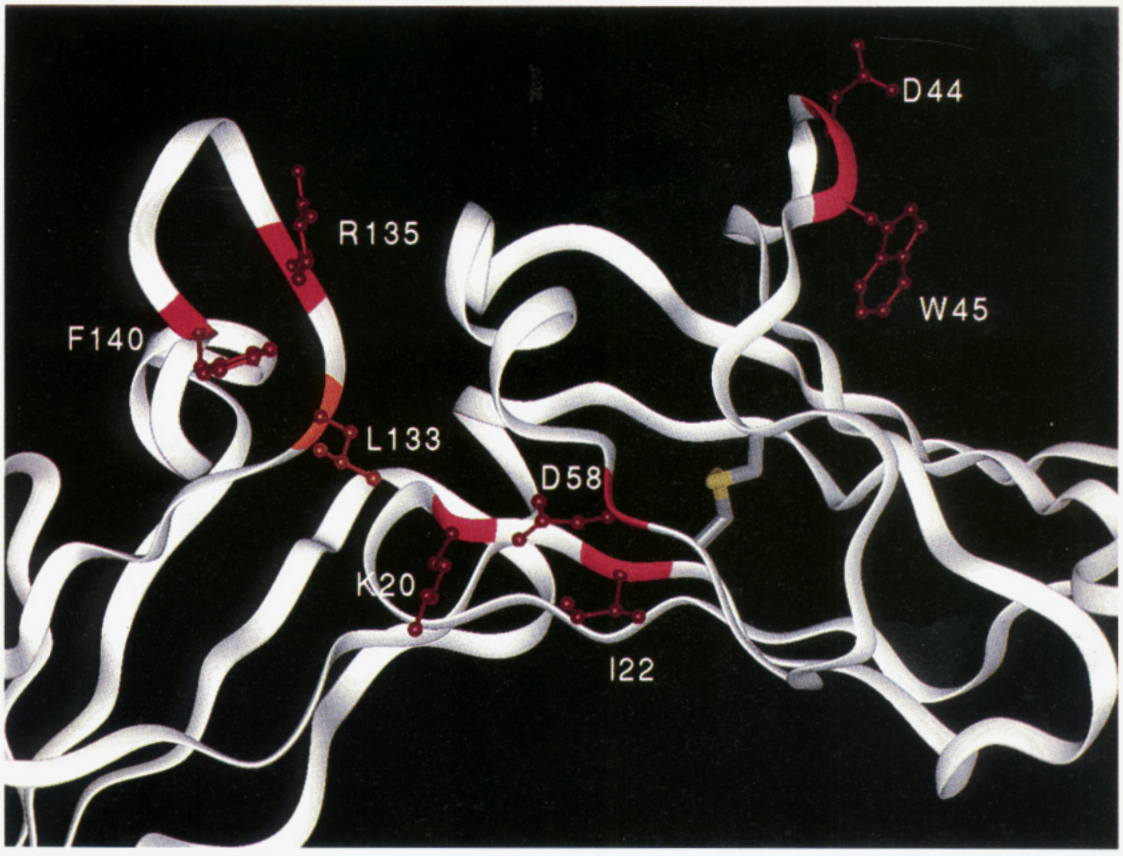

FIGURE 1: Ribbon representation of the module boundary of the extracellular domain of TF demonstrating the spatial relationship of Trp^{45} and Asp^{44} to previously identified binding residues [in bright red, Lys^{20}, Ile^{22}, Asp^{58}, Arg^{135}, Phe^{140} ($\Delta\Delta G$ > 0.5 kcal/mol); in light red, Leu^{133} ($\Delta\Delta G$ < 0.5 kcal/mol)].

Table 2: Functional K_{Dapp} Determination for Alanine Exchange Mutants in TF[a]

mutant	K_{Dapp} (pM)	calcd ΔG (kcal/mol)	$\Delta\Delta G$ (kcal/mol)	n
wild-type TF	2.6 ± 1.3	−16.4		8
Trp^{45}/Ser^{47}→Arg/Gly	31.7 ± 8.8	−14.8	1.6	3
Trp^{45}→Ala	32.7 ± 10.5	−14.8	1.6	5
Ser^{47}→Ala	2.1 ± 0.6	−16.5	−0.1	3
Val^{33}→Ala	1.9 ± 1.0	−16.6	−0.2	3
Tyr^{51}→Ala	2.1 ± 0.2	−16.5	−0.1	4
Phe^{76}→Ala	16.8 ± 3.7	−15.2	1.2	5
Tyr^{78}→Ala	7.5 ± 1.9	−15.7	0.7	4
Pro^{92}→Ala	1.9 ± 0.3	−16.6	−0.2	3
Tyr^{94}→Ala	4.4 ± 2.0	−16.1	0.3	4
Val^{36}→Ala	2.1 ± 0.6	−16.5	−0.1	3
Gln^{37}→Ala	8.9 ± 2.5	−15.6	0.8	5
Ile^{38}→Ala	2.1 ± 1.1	−16.5	−0.1	3
Gly^{43}→Ala	2.9 ± 1.5	−16.2	0.2	3
Lys^{48}→Ala	12.3 ± 1.6	−15.4	1.0	3
Cys^{49}/Cys^{57}→Ser	1.5 ± 0.6	−16.7	−0.3	3
Thr^{60}→Ala	111 ± 14	−14.1	2.3	4
Thr^{60}/Phe^{140}→Ala	3847 ± 546	−11.9	4.5	4
Thr^{60}/Lys^{20}→Ala	451 ± 94	−13.2	3.2	4
Asp^{44}→Ala	26.7 ± 5.9	−14.9	1.5	7
Asp^{44}/Trp^{45}→Ala	33.1 ± 3.4	−14.8	1.6	3
Asp^{44}/Phe^{140}→Ala	551 ± 185	−13.0	3.4	6
Asp^{44}/Lys^{20}→Ala	2206 ± 678	−12.2	4.2	5
Asp^{44}/Asp^{58}→Ala	1747 ± 706	−12.3	4.1	3
Asp^{44}/Thr^{60}→Ala	2905 ± 692	−12.0	4.4	4
$Asp^{44}/Lys^{20}/Phe^{140}$→Ala	41600 ± 13887	−10.4	6.0	5

[a] Mean and standard deviation are based on the given number of experiments (n). ΔG was calculated from the K_{Dapp} determined at 37 °C, and the change compared to wild-type TF is given as $\Delta\Delta G$.

binding of VIIa. The double mutant of Lys^{46}/Lys^{41} bound VIIa with slightly reduced affinity ($\Delta\Delta G$ < 0.5 kcal/mol), based on previous analysis (Ruf et al., 1994) consistent with a potential contribution of Lys^{46} to the ligand binding site. We had previously characterized the Cys^{49}/Cys^{57}→Ser mutant by radioligand assay (Rehemtulla et al., 1991) and concluded that binding of VIIa is normal. Identical results were obtained for the analysis of the mutant by the functional K_{Dapp} assay (Table 2), demonstrating that the disulfide bond and the exposed sulfur atom are not critical to maintain the functional conformation of the binding site. Binding of VIIa was reduced following Ala replacements for Gln^{37} but not when the buried adjacent residues Val^{36} and Ile^{38} were exchanged. The binding site further includes Lys^{48} with an estimated 1 kcal/mol contribution to the free energy of binding (Table 2), but residues Asp^{61} and Lys^{65} which form part of the surface of the intermodule cleft have been found to be dispensable for VIIa binding (Ruf et al., 1994).

Surprisingly, Ala replacement for Thr^{60}, which is largely buried under the nonfunctional Asp^{61} side chain (Figure 3), resulted in a substantial loss of binding function (Table 2). The binding defect of Thr^{60} mutation was completely independent of the Phe^{140} contact and partially additive with the mutation at Lys^{20}. Attempts to express the Asp^{58}/Thr^{60} double mutant at measurable levels in the eukaryotic cells failed, indicating that the Thr^{60} side chain may have some structural significance. The observed functional defect for the individual Thr^{60}→Ala exchange could thus reflect changes in the local packing of the binding interface at the module boundary. However, one cannot exclude interactions of the Thr^{60} side chain with ligand, if the nonfunctional Asp^{61} side chain reorients during ligand assembly.

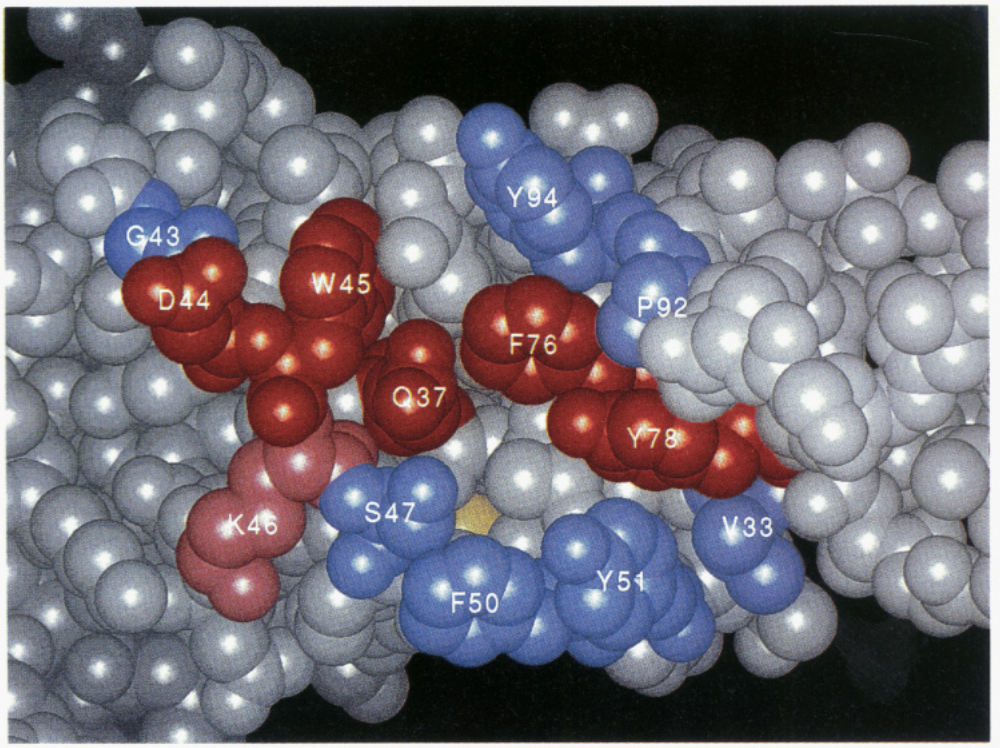

FIGURE 2: Space-filling representation of the surface of the hydrophobic patch in the amino-terminal module. Residues are colored according to their energetic contributions to VIIa binding: blue, $\Delta\Delta G \leq 0.3$ kcal/mol; red, $\Delta\Delta G > 0.5$ kcal/mol.

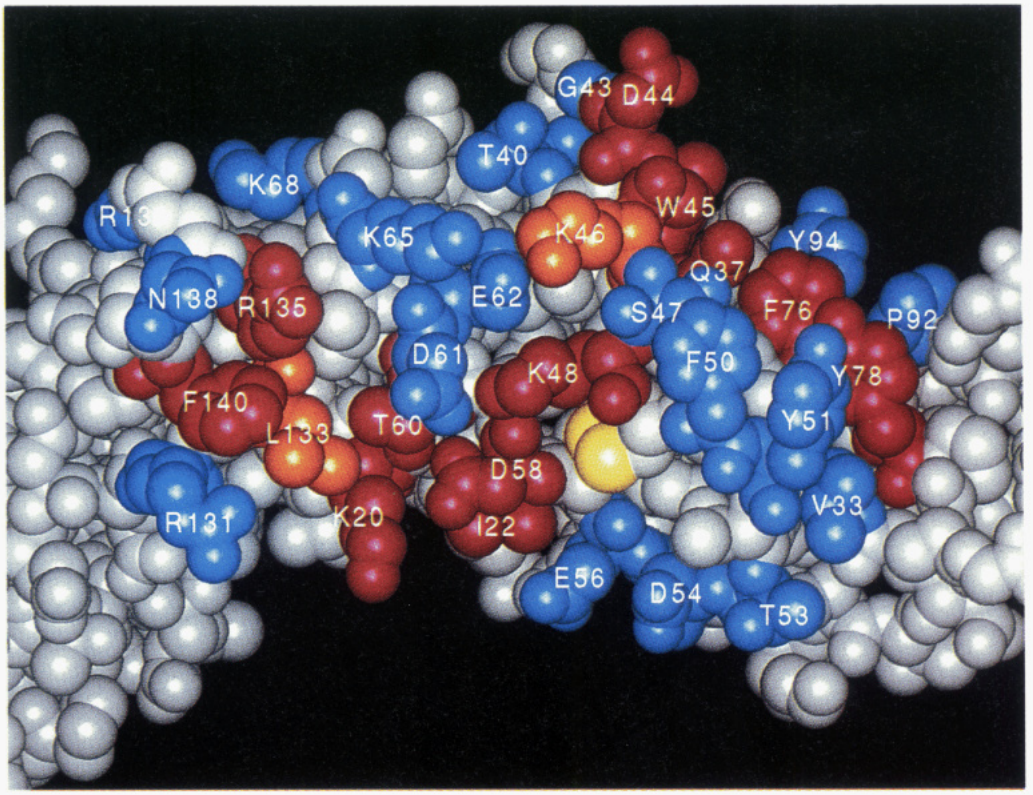

FIGURE 3: Overview of the ligand interactive area of TF in space-filling representation. Residues are colored according to their energetic contributions to VIIa binding: blue, $\Delta\Delta G \leq 0.3$ kcal/mol; orange, 0.3 kcal/mol $< \Delta\Delta G < 0.5$ kcal/mol; bright red, $\Delta\Delta G > 0.5$ kcal/mol.

Asp^{44}/Trp^{45} Represent an Independent Contact for VIIa. Asp^{44} is well exposed to solvent (Table 1) adjacent to the Trp^{45} aromatic side chain which packs tightly on the protein surface (Figure 2). The Asp^{44}/Trp^{45} double exchange mutant did not show additivity in the binding defect observed for the individual exchanges (Table 2), indicating a common reciprocal contact on VIIa. Alternatively, the Trp^{45} side chain may provide local structural support for the orientation of the Asp^{44} side chain, rather than directly interacting with ligand. We had not obtained evidence for global structural alterations of the Trp^{45}/Ser^{47}→Arg/Gly mutant (Rehemtulla et al., 1992). Similarly, antibody epitopes were expressed normally by the Asp^{44}→Ala exchange mutant (Figure 4). These data clearly exclude global conformational changes

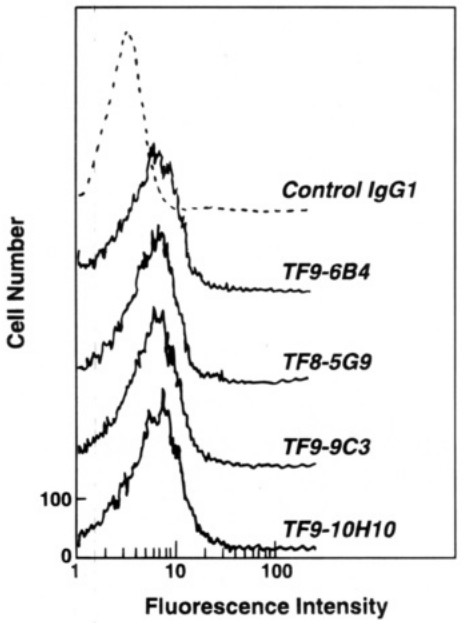

FIGURE 4: Analysis of monoclonal antibody epitope expression for the Asp[44]→Ala mutant by flow cytometry. The indicated primary antibodies were used at 30 μg/mL followed by fluorescent secondary antibody.

as a result of the mutations at these positions, consistent with the surface exposure of both residues.

The independence of the Asp[44]/Trp[45] contact from the cluster of binding residues at the module boundary was analyzed by determining the additivity of the mutational effect in a series of double replacement mutants. Asp[44] provided energetic contributions independent from the Lys[20], Asp[58], Thr[60], and Phe[140] side chains. Full additivity was further displayed by the Asp[44]/Lys[20]/Phe[140] triple mutant, clearly demonstrating that Asp[44] provides a contact which is unrelated to previously identified binding residues. This supports the overall conclusion that the binding site for VIIa significantly extends to the convex side on the amino-terminal module.

DISCUSSION

This study provides a structure-based analysis of the surface area of TF which is involved in interaction with the macromolecular ligand VIIa. Previously and newly identified ligand binding residues are found dispersed over a region which extends from the concave side of the elbow angle at the module boundary to the convex site on the amino-terminal module at the edge of the three- and four-stranded β-sheet (Figure 5). Most of the identified ligand binding residues are well exposed to solvent (Table 1), and the accessible surface area for the major contacts Lys[20], Ile[22], Gln[37], Asp[44], Trp[45], Lys[48], Asp[58], Phe[76], Tyr[78], Arg[135], and Phe[140] is 849 Å^2. The residue side chains of Tyr[51], Phe[50], Ser[47], Lys[46], Asp[61], Lys[65], and Leu[133] (Figure 3) provide continuity between the contact residues and have a combined accessible surface area of 686 Å^2. Under the assumption of continuity in the interface, in excess of 1500 Å^2 may be buried when VIIa assembles, and more than half of this area

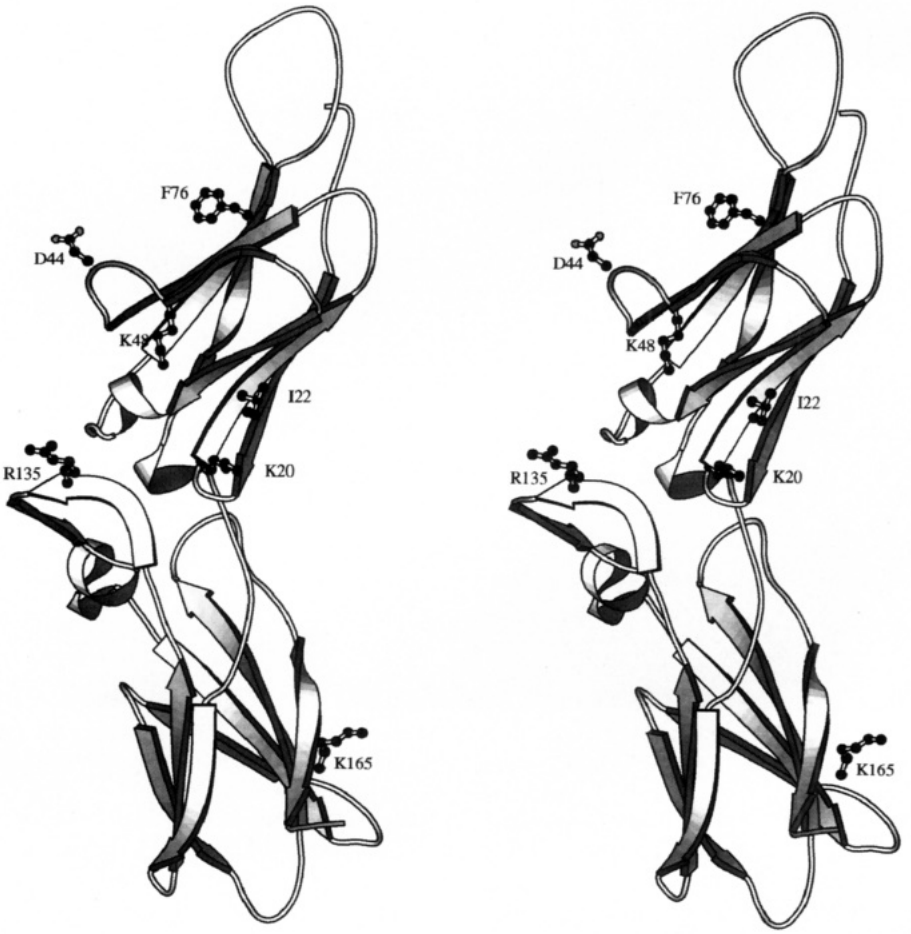

FIGURE 5: Stereo Molscript diagram of the TF extracellular domain. Critical residue side chains are displayed and labeled to show the extent of the ligand interactive region and its orientation to the structure important for activation of the macromolecular substrate marked by Lys[165].

would be involved in significant energetic contacts. This surface area is larger than to the buried interfaces of the homologous growth hormone receptor which are 900−1230 Å^2 (De Vos et al., 1992).

We here characterize the binding defect of TF mutants based on the K_{Dapp} determined by functional titration assay. The estimates for the energetic contributions based on this assay may deviate somewhat from the absolute change in the free energy of binding, because of the presence of the macromolecular substrate factor X which is used to monitor TF·VIIa complex formation. However, mutants of TF previously characterized by this assay had demonstrated similar quantitative alterations in binding of VIIa by subsequent analysis using other methodology (Gibbs et al., 1994; Muller et al., 1994), indicating that the overall conclusions from this analysis are valid. The ligand binding site is characterized by a fairly continuous cluster at the module interface which provides an estimated one-third of the free energy of binding (Schullek et al., 1994), and additional residues at the concave side of the elbow, such as Glu^{24} (Ruf et al., 1994) or Gln^{110} (Gibbs et al., 1994), may further contribute, possibly accounting for up to one-half of the free energy of binding. Additional contributions are provided by the residues in the extension of the binding site on the convex-shaped surface of the amino-terminal module. This area for ligand binding has not been appreciated in previous mapping of a limited number of binding residues on the structure of TF (Muller et al., 1994; Harlos et al., 1994). Antibodies directed to this region are potent inhibitors of VIIa binding to TF (Ruf et al., 1991b), further emphasizing the crucial role of this extension of the ligand binding site. The significant contacts of Lys^{48}, Asp^{44}, Phe^{76}, Tyr^{78}, and Gln^{37} account for an additional one-third of the binding energy, indicating that the majority of binding contacts are presented in this study. Although there is an apparent clustering of energetically significant residues at the module boundary, the binding residues appear to be dispersed over a fairly extended surface. This is in contrast to the growth hormone receptor in which two spatially close aromatic side chains provide the majority of the binding energy (Clackson & Wells, 1995).

The extended character of the TF ligand binding site might reflect adaptation to the multidomain ligand VIIa. Light chain modules of VIIa (Higashi et al., 1994; Toomey et al., 1991; Clarke et al., 1992; Kazama et al., 1993; O'Brien et al., 1994; Ruf et al., 1991a) and the protease domain (Higashi et al., 1994; O'Brien et al., 1991; Matsushita et al., 1994) are involved in the interaction with TF. The groove-like shape of the module boundary and the convex surface surrounding Asp^{44} and the hydrophobic patch could provide the necessary shape complementarity for interaction with these structurally diverse modules of VIIa. The VIIa binding site on TF is located mostly at the opposite side relative to Lys^{165} and Lys^{166} (Figure 5), which are critical residues for activation of macromolecular substrates without affecting the interaction with VIIa (Ruf et al., 1992). It is presently unknown how VIIa docks with TF to present the active site for efficient recognition of the macromolecular substrates factors X and IX. The detailed insight into the structural basis for function of the TF ligand binding site provided here will further future studies to address the more complex questions of macromolecular assembly of substrate with the enzyme−cofactor complex.

ACKNOWLEDGMENT

We thank Cindi Biazak, David Revak, and Pablito Tejada for excellent technical assistance and Barbara Parker for preparation of the manuscript. We also thank Adam Wacey for his assistance in producing the molecular graphics figures.

REFERENCES

Clackson, T., & Wells, J. (1995) *Science 267*, 383−386.
Clarke, B. J., Ofosu, F. A., Sridhara, S., Bona, R. D., Rickles, F. R., & Blajchman, M. A. (1992) *FEBS Lett. 298*, 206−210.
Davie, E. W., Fujikawa, K., & Kisiel, W. (1991) *Biochemistry 30*, 10363−10370.
De Vos, A. M., Ultsch, M., & Kossiakoff, A. A. (1992) *Science 255*, 306−312.
Gibbs, C., McCurdy, S., Leung, L., & Paborsky, L. (1994) *Biochemistry 33*, 14003−14010.
Harlos, K., Martin, D. M. A., O'Brien, D. P., Jones, E. Y., Stuart, D.I., Polikarpov, I., Miller, A., Tuddenham, E. G. D., & Boys, C. W. G. (1994) *Nature 370*, 662−666.
Higashi, S., Nishimura, H., Aita, K., & Iwanaga, S. (1994) *J. Biol. Chem. 269*, 18891−18898.
Kabsch, W., & Sander, C. (1983) *Biopolymers 22*, 2577−2637.
Kazama, Y., Pastuszyn, A., Wildgoose, P., Hamamoto, T., & Kisiel, W. (1993) *J. Biol. Chem. 268*, 16231−16240.
Matsushita, T., Kojima, T., Emi, N., Takahashi, I., & Saito, H. (1994) *J. Biol. Chem. 269*, 7355−7363.
Muller, Y. A., Ultsch, M. H., Kelley, R. F., & De Vos, A. M. (1994) *Biochemistry 33*, 10864−10870.
O'Brien, D. P., Gale, K. M., Anderson, J. S., McVey, J. H., Miller, G. J., Meade, T. W., & Tuddenham, E. G. D. (1991) *Blood 78*, 132−140.
O'Brien, D. P., Kemball-Cook, G., Hutchinson, A. M., Martin, D. M. A., Johnson, D. J. D., Byfield, P. G. H., Takamiya, O., Tuddenham, E. G. D., & McVey, J. H. (1994) *Biochemistry 33*, 14162−14169.
Rehemtulla, A., Ruf, W., & Edgington, T. S. (1991) *J. Biol. Chem. 266*, 10294−10299.
Rehemtulla, A., Ruf, W., Miles, D. J., & Edgington, T. S. (1992) *Biochem. J. 282*, 737−730.
Ruf, W., & Edgington, T. S. (1994) *FASEB J. 8*, 385−390.
Ruf, W., Kalnik, M. W., Lund-Hansen, T., & Edgington, T. S. (1991a) *J. Biol. Chem. 266*, 15719−15725.
Ruf, W., Rehemtulla, A., & Edgington, T. S. (1991b) *Biochem. J. 278*, 729−733.
Ruf, W., Miles, D. J., Rehemtulla, A., & Edgington, T. S. (1992) *J. Biol. Chem. 267*, 6375−6381.
Ruf, W., Miles, D. J., Rehemtulla, A., & Edgington, T. S. (1993) *Methods Enzymol. 222*, 209−224.
Ruf, W., Schullek, J. R., Stone, M. J., & Edgington, T. S. (1994) *Biochemistry 33*, 1565−1572.
Schullek, J. R., Ruf, W., & Edgington, T. S. (1994) *J. Biol. Chem. 269*, 19399−19403.
Toomey, J. R., Smith, K. J., & Stafford, D. W. (1991) *J. Biol. Chem. 266*, 19198−19202.
Waxman, E., Ross, J. B. A., Laue, T. M., Guha, A., Thiruvikraman, S. V., Lin, T. C., Konigsberg, W. H., & Nemerson, Y. (1992) *Biochemistry 31*, 3998−4003.

BI942623T